Machined silicon traps for capturing novel bacterial communities and strains *in-situ*

Clara Romero Santiveri,[†] Joseph H. Vineis,[‡] Sofia Martins,[¶] Carlos Calaza,[¶] João Gaspar,[¶] Jennifer L. Bowen,[*,‡] and Edgar D. Goluch[*,†]

†*Department of Chemical Engineering, Northeastern University, Boston, Massachusetts*

‡*Department of Marine and Environmental Sciences Marine Science Center, Northeastern University, Nahant, Massachusetts*

¶*International Iberian Nanotechnology Laboratory, Braga, Portugal*

E-mail: je.bowen@northeastern.edu; e.goluch@northeastern.edu

Phone: +1-617-373-3500

Abstract

We tested the feasibility of a novel machined silicon nanopore enrichment device to recover individual microbial taxa from anaerobic sediments. Unlike other environmental isolation devices that have multiple entry points for bacteria or require the sample to be manually placed inside of a culturing chamber, our silicon device contains 24 precisely sized and spaced nanopores, each of which is connected to one culturing well, thereby providing only one entry point for bacteria. The culturing wells allow nutrient transport, so the bacteria that enter continue to experience their natural chemical environment, allowing collection of microbes without manipulating the environment. The device was deployed in marsh sediment and subsequently returned to the laboratory for bacterial culturing and analysis. 16S rRNA marker gene and metagenomic sequencing was used to quantify the number of different microbial taxa cultured from the device. The 16S rRNA sequencing results indicate that each well of the device contained between 1 and 62 different organisms from several taxonomic groups, including likely novel taxa. We also sequenced the metagenome from 8

of the 24 wells, enabling the reconstruction of 56 metagenomic assembled genomes (MAGs), and 44 of these MAGs represented non-redundant genome reconstructions. These results demonstrate that our novel silicon nanofluidic device can be used for isolating and culturing consortia containing a small number of microbial taxa from anaerobic sediments, which can be very valuable in determining their physiological potential.

Importance

There are very few methods that can remove a few bacterial cells from a complex environment and keep the cells alive so that they can propagate sufficiently to be analyzed in a laboratory. Such methods are important to develop because the physiological functions of individual species of bacteria are often unknown, cannot be determined directly in the complex sample, and many bacterial cells cannot be grown outside of their natural environment. A novel bacterial isolation device has been made tested in a salt marsh. The results show that the device successfully isolated small groups of bacterial species from the incredibly diverse surroundings. The communities of bacteria were easily removed from the device in the laboratory and analyzed.

Introduction

Microorganisms are the most diverse forms of life on Earth. There are 100 million times as many bacterial cells in the oceans (13×10^{28}) as stars in the known universe [1]. Despite the astonishing progress in microbiology over the past century, we have only scratched the surface of this enormous microbial world. It has been estimated that <1% of bacterial species have been cultured in the laboratory [2]. Based on sampling location, ~1% of sediment bacteria, 0.01-0.1% of soil bacteria, and 0.001-0.1% of marine (surface) bacteria have been cultivated in the laboratory [3]. To improve and accelerate bacterial cultivation, microfluidic devices with various configurations have been developed for sorting, isolating, and studying microorganisms (Table 1).

However, most microfluidic devices require sophisticated external instrumentation to be operated (active microfluidics) and, therefore, need to remove the sample from the original environment for processing, which potentially introduces sample bias and loss of diversity [4-8]. These active microfluidic techniques manipulate the particles' movement in real-time by using external forces, including electric fields [9-12], acoustic streaming [13], magnetic fields [14-15].

A few passive sorting microfluidic devices have been demonstrated, but only a few do not disturb the environment. The iChip, for example, has been successfully used to cultivate many new species of bacteria, however, the sample must be collected by the user, diluted, the cells then placed inside of the isolation chambers, prior to placing it into the environment for nutrient exchange [16-18]. Completing these steps in the field is cumbersome, and placement of the device back in exact location, to the millimeter, where the sample was collected is nearly impossible. Rezaei *et al.* designed an ingestible pill device recently, which does not disturb the environment as it takes samples from the gut after being swallowed [25]. However, the purpose of the device is different. The ingestible pill is intended for sampling of gut microbiota and it does not limit the bacterial diversity that is collected.

Tandogan *et al.* developed a polymer nanofluidic device, a predecessor of the device demonstrated in this article, which used a similar design with sub-micrometer channel features to limit bacterial cell access isolation chambers [24]. Our device overcomes several limitations from the previous version. Anaerobic bacteria can now be cultured using silicon wafers and polycarbonate as the central part of the trap instead of polydimethylsiloxane (PDMS), which is gas permeable. The constrictions in our device are exposed directly to the environment sample without the bacteria needing to enter the main channel before getting to the constrictions, whereas the PDMS device required that the bacterial cells travel nearly a centimeter to reach the nanochannel. Finally, and most importantly, the silicon nanopore

devices can be manufactured in volume using established microfabrication techniques borrowed from the microelectronics industry.

Isolation process	References	Microfluidic type	Does it disturb the environment?
Droplet-based	Watterson *et al.* (2020) [4]	Active	Yes
	Eun *et al.* (2011) [5]		
	Villa *et al.* (2019) [6]		
	Leung *et al.* (2012) [7]		
Pressure-driven	Bamford *et al.* (2017) [8]	Active	Yes
Dielectrophoresis	Lu *et al.* (2013) [9]	Active	Yes
	Jiang *et al.* (2019) [10]		
	D'Amico *et al.* (2017) [11]		
	Braff *et al.* (2013) [12]		
Acoustophoresis	Dow *et al.* (2018) [13]	Active	Yes
Magnetic beads	Chang *et al.* (2014) [14]	Active	Yes
	Miller *et al.* (2019) [15]		
Dilution	Nichols *et al.* (2010) [16]	Active	Yes
	Yoshiteru *et al.* (2009) [17]		
	Berdy *et al.* (2017) [18]		
Microfiltration	Raub *et al.* (2015) [19]	Passive	Yes
	Fan *et al.* (2015) [20]		
Selective lysis	Zelenin *et al.* (2015) [21]	Passive	Yes
Inertial (flows)	Wu *et al.* (2009) [22]	Passive	Yes
Chemotaxis	Männik *et al.* (2009) [23]	Passive	Yes
	Tandogan *et al.* (2014) [24]		No
	Rezaei *et al.* (2019) [25]		No
	Our device		No

Table 1. Summary of articles that used different microfluidic-based approaches for cell sorting and isolation..

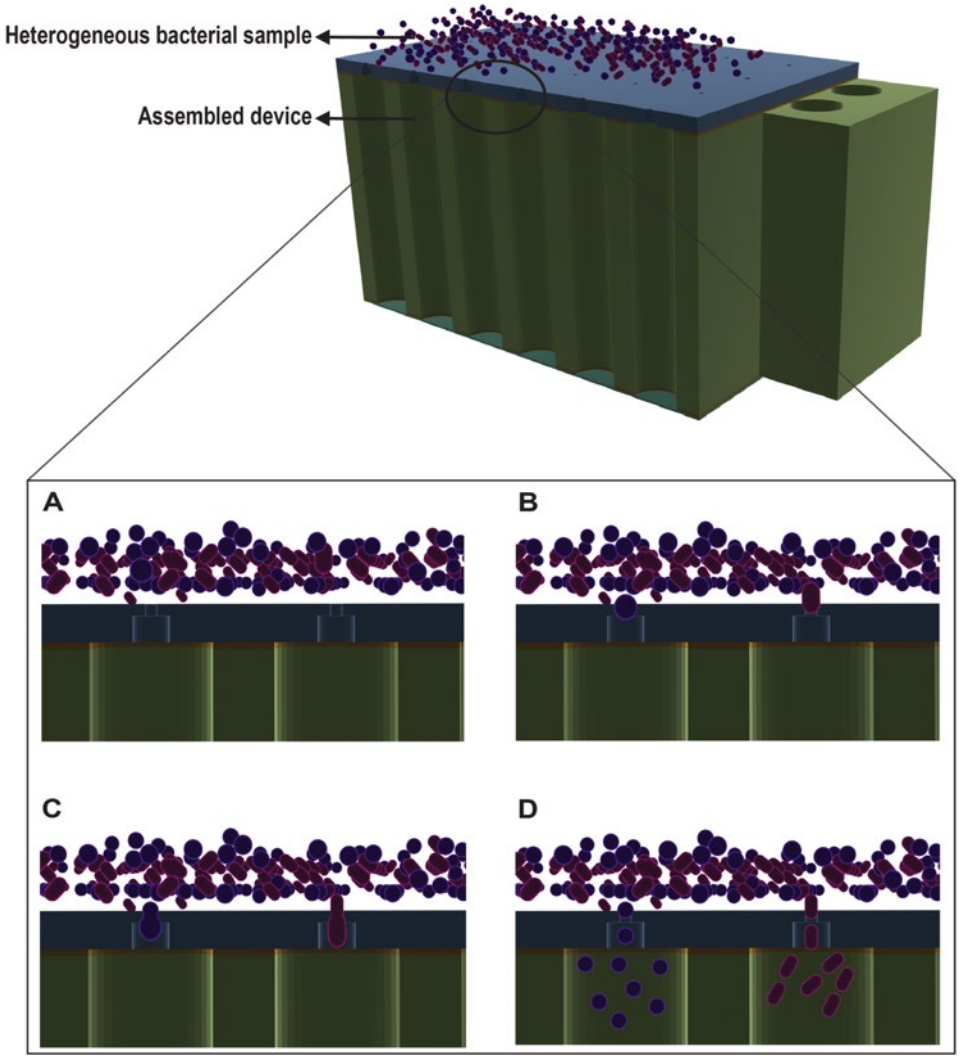

Figure 1. Schematic of the microfluidic device. The wafer is connected to the isolation chambers via nano- and sub-micron constrictions. Heterogeneous bacterial culture self-sort into different isolation chambers with the help of chemotaxis and size-specific constrictions.

Here, we describe a novel, passive, nanofabricated device that allows for in-situ isolation of bacterial species. The isolated bacteria are exposed to nutrients in their natural surroundings using a nanoporous membrane. Thus, the device eliminates the need for sample processing before initiating a culture and provides the opportunity to perform genomic analysis on cells obtained directly from natural communities.

A silicon single-side polished (SSP) wafer and a silicon on insulator (SOI) wafer are used as the base of the device; it has 24 holes (constrictions) that vary in diameter, they range from 2 µm to 0.5 µm on the SSP and from 1.1 µm to 0.1 µm on the SOI wafer. These constrictions are at least

one dimension smaller than the diameter of a bacterial cell. Fresh food in the isolation chambers chemotactically attracts microorganisms toward the constrictions (Figure 1). As a result, bacterial species get trapped at the entrance of these sub-micron constrictions (Figure 1B), preventing other bacterial cells from reaching the isolation chamber. The trapped microorganism continues to divide (Figure 1C), and each progeny advances further through the constriction. Finally, after several successions, only one species will enter the isolation chamber, which is the predecessor of the trapped species (Figure 1D).

Microbial diversity and community composition is assessed using 16S ribosomal RNA (rRNA) sequencing. This technique has allowed the discovery of important relationships between microbial structure and function and led to the discovery of the "rare biosphere" [26]. However, estimates of diversity and species counts can be heavily influenced by the differences in the number of 16S rRNA operons within individual organisms [27], polymerase chain reaction (PCR) errors, sequencing errors [28], and primer bias [29]. Genome reconstruction from metagenomic data can provide a less biased representation of the diversity of a community because the preparation of samples requires fewer PCR cycles, avoids primer bias, and analytical approaches are not influenced by the operon structure of individual marker genes. This approach also allows us to identify the metabolic potential of microbial organisms within the environment. However, the immense diversity of natural communities hampers our ability to reconstruct all microbial genomes from most environmental samples.

While dilution to extinction and enrichment cultures are commonly used to overcome this problem, they are generally conducted within the laboratory under purely synthetic conditions. The ability to isolate a reduced community or individual strains *in-situ* significantly increases the opportunity for microbiologists to identify novel microbial metabolism and interactions. *In-situ* isolation can also improve current laboratory cultivation yield because the metabolic handoffs and environmental conditions relied upon by many taxa for growth are preserved. Further, pure bacterial cultures are essential for understanding investigating virulence factors, antibiotic susceptibility, and genome sequences. However, only a few bacterial species can be cultivated by

routine culture, so molecular analyses of environmental sequences are employed to substantially expand our knowledge of microbial life [30], [31].

Materials and Methods

Wafer Fabrication

The micromachining of silicon-on-insulator (SOI) wafer substrates was performed using a SiO2 hard mask for the silicon dry etching process. A 1.5 µm thick SiO2 layer was first deposited on the front side of the SOI substrate using a plasma-enhanced chemical vapor deposition (PECVD) system (MPX from SPTS). Direct write laser lithography (DWL 2000 from Heidelberg Instruments) with a 1.2 µm thick AZP4110 positive photoresist was then used to define the geometry of the small constrictions on the front side. The layout consisted of a 6x4 matrix of circular constrictions with diameters ranging from 1.50 µm to 2.25 µm. The layout was repeated 28 times on an 8-inch-diameter wafer. After exposure, the resist was developed using AZ400K.

The SiO_2 layer was then patterned by reactive ion etching (RIE) using a C_4F_8 based plasma in an APS reactor from SPTS. Next, 10-µm-deep circular constrictions were achieved using deep reactive ion etching (DRIE) of silicon (Pegasus system from SPTS) using a SF_6/C_4F_8 etching chemistry. The resist mask was then stripped using an oxygen plasma etch (PVA GIGAbatch 360 M tool from Tepla).

The backside of the wafer was micromachined as well to achieve through-wafer channels. First, a 5-µm-thick PECVD SiO_2 layer was deposited on the back of the wafer. This layer acted as a hard mask for the subsequent DRIE step. Next, lithography for the patterning of through-wafer channels was performed on a Mask Aligner system (MABA6 from SussMicroTec) using a 2.2 µm thick AZP4110 positive photoresist. The layout consisted of a 6x4 matrix of circular holes with a diameter of 25 µm, aligned with the previous frontside lithography and repeated 28 times. After exposure, the resist was developed using AZ400K.

The processes used for both the etching of the SiO_2 hard mask and the resist strip are similar to those previously used on the front side. Before the DRIE process, a thermal release tape was applied on the wafer's front side to prevent leakage through the front side constrictions in the event of breakage on the SOI buried oxide layer (BOX). The through-wafer channels with 725 µm depth were obtained with a DRIE process using a SF_6/C_4F_8, which stopped on the BOX layer. Then the thermal release tape was removed by placing the wafer on a hotplate at 180 ºC, and channels were opened by removing the exposed BOX layer using an HF vapor tool (Primaxx from SPTS).

The size of the small constrictions can be tailored for different applications. For example, if narrower constrictions are required, a new PECVD SiO_2 layer can be deposited to reduce the effective diameter of the SiO_2. A 2.1-µm-thick layer was deposited in this case to obtain constrictions with dimensions in the range of 0.25 µm - 1.25 µm.

Dicing the wafers into 28 individual devices containing the 6x4 array of channels without damaging the small constriction structures was a uniquely challenging step. This process was completed by assembling a protection thermal release tape on the front side and a regular dicing tape on the backside of the wafer and performing the dicing from the front side. Dicing tape was then released with UV exposure for a few minutes and front side tape using heating the wafer in an oven at 180 ºC. A process diagram for device fabrication is provided in the Supporting Information as Figure S1.

A silicon single-side polished (SSP) wafer and a silicon on insulator (SOI) wafer are used as the base of the device; it has 24 holes (constrictions) that vary in diameter, they range from 2µm to 0.5µm on the SSP and from 1.1µm to 0.1µm on the SOI wafer.

The final wafer can be divided into rows; there are four rows with six constrictions on each row (Figure 2) ad each row has different constriction diameter (Table 2). The SSP wafer constriction diameters range from 2.0 µm to 0.5 µm while the SOI wafer diameters range from 1.0 µm to 0.1 µm.

Figure 2. Arrangement of constrictions on a silicon device.

Wafer	A	B	C	D
SSP	2µm	1.4µm	1µm	0.5µm
SOI	1.1µm	0.7µm	0.4µm	0.1µm

Table 2. Constriction diameters.

Device Assembly

The device consists of 4 elements (Figure 3): the wafer, two double-sided adhesives (Adhesive Transfer Tape Acrylic Adhesive Clear, DigiKey), a polycarbonate body (Clear Impact-Resistant Polycarbonate, McMaster-Carr), and a Nuclepore track-etched polycarbonate (PC) membrane

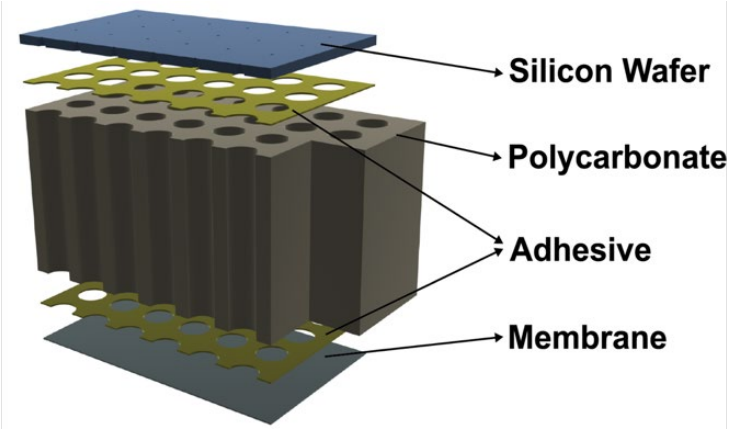

Figure 3. Schematic identifying the parts off the silicon trap.

(0.05 µm pore size, Whatman). Before assembling the final device, the adhesive was cut using an Epilog Zing laser cutter (30W). Next, circles were cut in the double-sided adhesive so that there was an open path between the channels in the wafer and the wells in the polycarbonate and between the wells and the nanoporous membrane. Finally, the nanoporous membrane was manually cut to match the size of the polycarbonate part.

After autoclaving all of the components, the double-sided adhesive was first adhered to the polycarbonate body aligning the holes and wells. Then, one side of the polycarbonate, the rough

backside of the wafer, was attached to the polycarbonate, while the smooth front side was exposed to the environment. Finally, the wafer and the plastic part were designed to align correctly using hand positioning.

Next, the device was filled with liquid medium, and finally, the nanoporous membrane was attached to the polycarbonate body using a second piece of double-sided adhesive. The membrane pore size is small enough to block bacterial cells from entering the isolation well but wide enough to allow diffusion of nutrients into the device to cultivate the trapped bacteria.

Cultivar Collection

A single trap consisting of 24 chambers, basic marine medium (Gibco), a polycarbonate membrane, and the silicon wafer were autoclaved, sterilized, and placed into an anaerobic chamber (Coy) containing 95% N_2 and 5% H_2 gas in the presence of a Stak-Pak catalyst for 48 hrs to remove O_2.

Nitrate was added to the medium after sterilization to a final concentration of 1000 µM. After attaching the bottom of the trap with adhesive, we added approximately 50 µL of medium to each well before adding the nutrient permeable membrane on the top. The trap was placed into a 50 mL conical tube filled with the same medium and transported to Plum Island Long Term Ecological Research (LTER) Site, approximately 1 hr away from the Northeastern University Marine Science Center. A soil core (8 x 40 cm) was taken from the sediment of the short ecotype of *Spartina alterniflora* on the high marsh platform. A sterile razor blade was used to make an incision approximately 4 cm deep along the core length. The device was embedded into the core at 35 cm from the surface, and the entire core was returned to its original position and allowed to incubate for 10 days. After the incubation period, the traps and surrounding sediment were recovered, placed into a plastic bag, and transferred to an anaerobic chamber within an hour. The trap was rinsed with sterile deionized water and cleaned with 70% ethanol using a Kimwipe. A sterile 1 ml syringe was used to transfer the entire contents of each well to separate Hungate tubes containing 10 mL of sterile basic marine medium. Several Hungate tubes containing medium were not inoculated to

serve as negative controls. Growth was determined by turbidity and the presence of black particulates in the medium that likely resulted from sulfur-driven iron reduction.

DNA purification

After 21 days of growth in the Hungate tubes, we purified DNA from 1 mL of cells and medium using a sucrose lysis buffer approach adapted from Britschgi and Fallon 1994 [32]. In addition, duplicate DNA extractions were completed for four of the samples to assess extraction and PCR bias.

16S amplification and ASV clustering

Partial 16S rRNA gene sequences were amplified from the purified DNA according to Caporaso et al. [33] and sequenced on a MiSeq using 2 x 250 PE v2 chemistry. Reads were quality filtered, merged, and clustered into amplicon sequence variants (ASVs) using the Dada2 pipeline v 1.14.0.[39].

Metagenomic library construction and MAG reconstruction

Metagenomic libraries were constructed for eight of the cultures that displayed unique combinations of ASVs. We sheared approximately 1 µg of purified DNA as input for the NuGen Ovation R DNA library prep kit and followed the recommendations of the protocol to create all libraries. Each library was quantified using the Invitrogen pico-green DNA assay, and we pooled all eight libraries based on the picogreen concentrations in an equimolar fashion. We size selected the pooled libraries to 600 bp using a Covaris ME220 ultrasonicator according to the manufacturer's recommendations. The library was cleaned using AMPure XP R DNA purification beads at a 1:1 DNA to bead ratio. We quantified the final library using a Kapa qPCR Illumina library quantification kit to optimize the concentration of the library for sequencing. The library was sequenced on an Illumina MiSeq according to PE 2 x 250 v3 chemistry. All reads were quality filtered using Illumina-utilities v2.6 using the default parameters of "iu-filter-minoche" [35]. Filtered reads were assembled into contigs using the SPAdes genome assembler v3.13.0 [36]

188 according to the metagenomic pipeline. Finally, we mapped the short reads from each of the eight
189 samples onto each of the individual assemblies using bowtie2 v 2.2.9 [37].

190 We used Anvi'o v 6.1 [38] to reconstruct genomes from the assembled metagenomic data. We
191 began by creating a contigs database using the command "anvi-gen-contigs-database," which
192 included identification of open reading frames (ORFs) using Prodigal [39], calculation of contig
193 tetranucleotide frequency, and splitting contigs larger than 20 kbp into 10 kbp "splits." The
194 command "anvi-run-hmms" searched all contigs for the presence of single-copy genes using three
195 separate collections, including bacterial, archaeal, and eukaryotic collections. This algorithm uses
196 HMMER as the search engine to identify the presence of single-copy gene collections [40]. To link
197 the mapping data for each sample to the contigs database, we used the command "anvi-profile."
198 All profile databases were merged using "anvi-merge," and we used a manual approach employed
199 by "anvi-interactive" to place contigs into bins that were most similar in coverage profiles across
200 all samples.

201 The interactive interface of Anvi'o also allowed us to evaluate the percentage of single-copy
202 genes detected and those that were redundant in the collection of contigs to more accurately place
203 contigs into MAGs. Filtered sequencing reads are contained within NCBI under the project
204 PRJNA714626. The specifications of each command can be found here
205 (https://github.com/jvineis/Enrichment-Traps), and the files required to visualize the selection of
206 contigs can be found here (https://doi.org/10.6084/m9.figshare.13650800). We created a list of
207 non-redundant MAGs based on their average nucleotide identity (ANI) using two steps. First, we
208 ran "anvi-compute-genome-similarity" to calculate the pairwise percent identity and the percent
209 alignment of all MAGs. Then we used "anvi-dereplicategenomes" to identify MAGs that contained
210 95% ANI across 90% of their genome, specifying the use of pyANI [41]. Finally, we identified
211 MAG taxonomy using "anvi-run-scg-taxonomy," which uses DIAMOND [42] to search single-
212 copy genes identified in the MAGs to reference sequences in the Genome Taxonomy Database
213 (GTDB) [43].

Estimating MAG relative abundance

Following MAG reconstruction and dereplication, we exported a fasta file for each split in the collection of MAGs and mapped each of the short read metagenomic datasets back to this fasta file using bowtie2. We converted the resulting sam file to a bam file and removed all alignments with a MAPQ score below 10 using "samtools view." Removal of alignments below this threshold is an effective way to remove non-specific alignments and reads that map to more than one position. However, multiple alignments for individual reads can still be retained using this method which can slightly influence relative abundance estimates. We tabulated the number of reads that were recruited to each split using "samtools idxstats" and a custom script to tabulate the number of reads for each MAG.

Results and Discussion

The 16S rRNA sequencing effort produced an average of 22,879 high-quality reads per sample with a minimum of 14,513 and a maximum of 28,780 (Figure 4). A total of 185 unique ASVs were detected, and the number of ASVs per sample ranged from 1 to 62, with a mean of 23 (Figure S2). The technical replicate amplicon processing from four samples (indicated by colored boxes at the bottom of Figure 4) indicates that the results are robust for separate DNA extractions of the same culture.

The diversity of ASVs within the wells of the trap can be broken down into three major groups. In the first group (trap well numbers 22, 6, 23, 24, and 20), a single ASV most closely related to *Vibrionaceae* represented more than 94% of all sequences (Figure 2). In two of the trap wells (22 and 6), this ASV represented more than 99% of all sequences. The second group, representing four

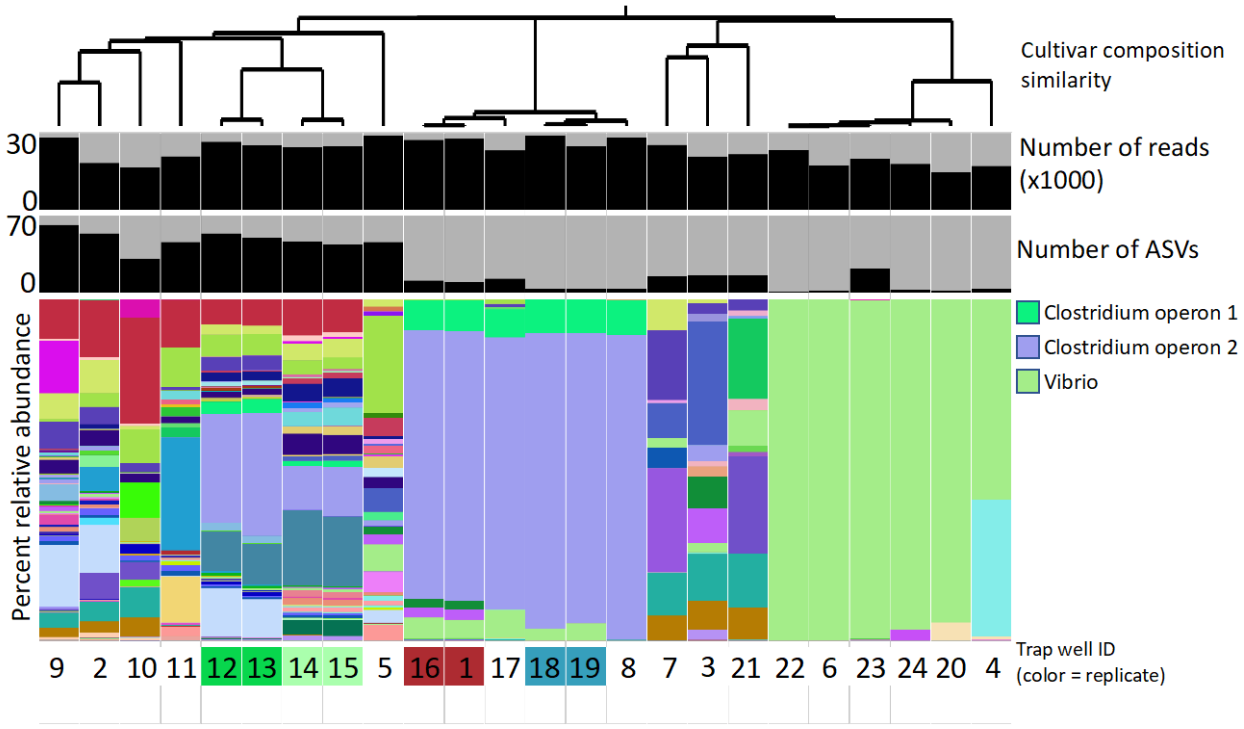

Figure 4. Summary of ASVs detected in trap wells, including a hierarchical tree showing the relationship in ASV composition among each of the trap wells (top). Barplots include the number of quality filtered reads per sample (top) the number of ASVs (middle), and the percent relative abundance of each ASV within each of the trap wells (bottom). The number at the bottom of the figure indicates the ID of the well. The presence of color behind the number indicates if the sample was a technical replicate and if two boxes have the same color then the DNA was extracted from the same cultivar.

of the trap wells (17, 18, 19, and 8), is dominated by two ASVs that are likely operons derived from the same organism with taxonomic resolution to *Clostridiales*. An alignment of the two representative sequences for the *Clostridiales* ASVs indicated that there was a single nucleotide difference between them, and they occurred at a 9:1 ratio within all samples where they were detected. The two ASVs combined to reach greater than 85% of all sequences in four of the trap-wells. The third group was comprised of trap wells containing a diversity of bacterial taxa. Within this group, there were 127 ASVs that occurred in less than three samples, and 87 of these were never detected above 5% in any of the trap wells (Figure S2, Table S1). The remaining 55 ASVs occurred in three or more samples, and the mean percent relative abundance for this group of ASVs was 3.8. Twelve ASVs that occurred in more than two wells had a mean of 5 percent relative abundance (Figure 4, Figure S2, Table S1). These results indicate that there was significant overlap

246 in the cultured organisms isolated from many of the trap wells, which is surprising given the large
247 amount of diversity that exists within salt marsh sediments [44], [45].

248 We reconstructed a total of 56 draft genomes of medium to high quality according to MIMAG
249 standards [46] from eight of the trap wells. Dereplication of these MAGs produced a set of 44
250 unique MAGs (Table S2).

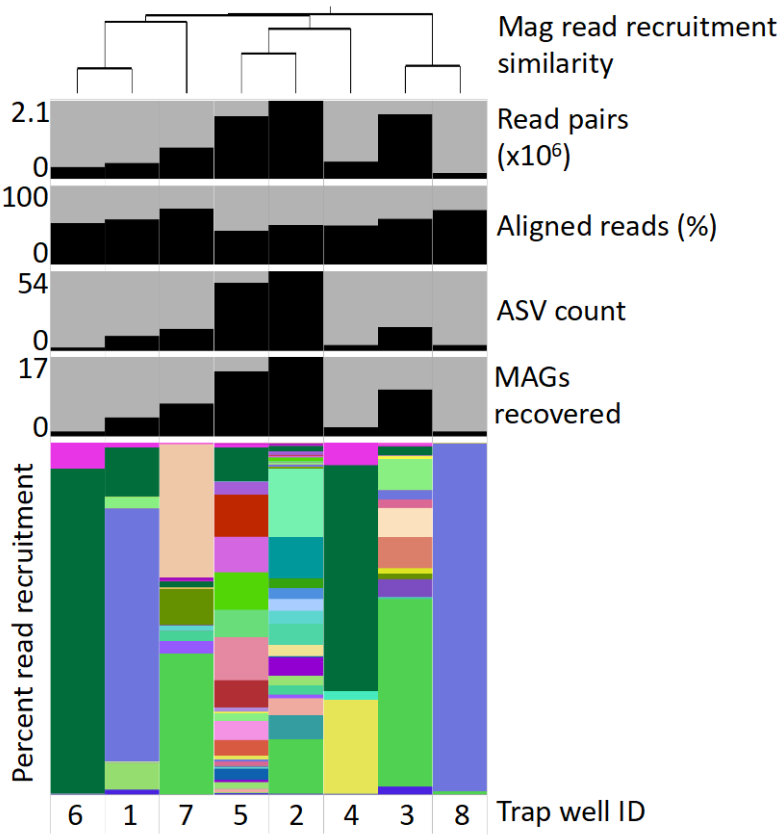

Figure 5. Summary of metagenomic assembled genomes (MAGs) from eight trap wells ordered by the hierarchical tree (top) based on the similarity in relative percent read recruitment of all MAGs. Bar plots, from top to bottom indicate 1) the number of quality filtered read pairs per sample, 2) the number of reads that align to the non-redundant collection of MAGs, 3) the number of ASVs detected in the sample, 4) the number of MAGs recovered from each sample, and 5) the percent relative abundance of each non-redundant MAG in each of the cultivars. The trap wells are identified at the bottom of the figure.

251 In trap well #8, where ASV analysis indicated the presence of a dominant organism closely
252 related to *Vibrio*, a single MAG was resolved with completion and redundancy scores of 100%
253 and 0%, respectively, with 68% of all short reads recruiting back to the MAG and consistent
254 coverage across all contigs with the exception of a contig containing 16s rRNA genes (Figure 5).

255 Two additional MAGs with 95% ANI across 90% of their genome were recovered from two other
256 wells and likely represented organisms from the same population (Figure 5). In trap wells with a
257 greater diversity of organisms, we recovered up to 17 MAGs with over 50% read recruitment in
258 nearly all samples (Figure 5).

259 We observed minimal variability in alignment of short reads too many of the MAGs in this
260 study (Figure 6), indicating that in most cases, we were able to isolate individual strains.

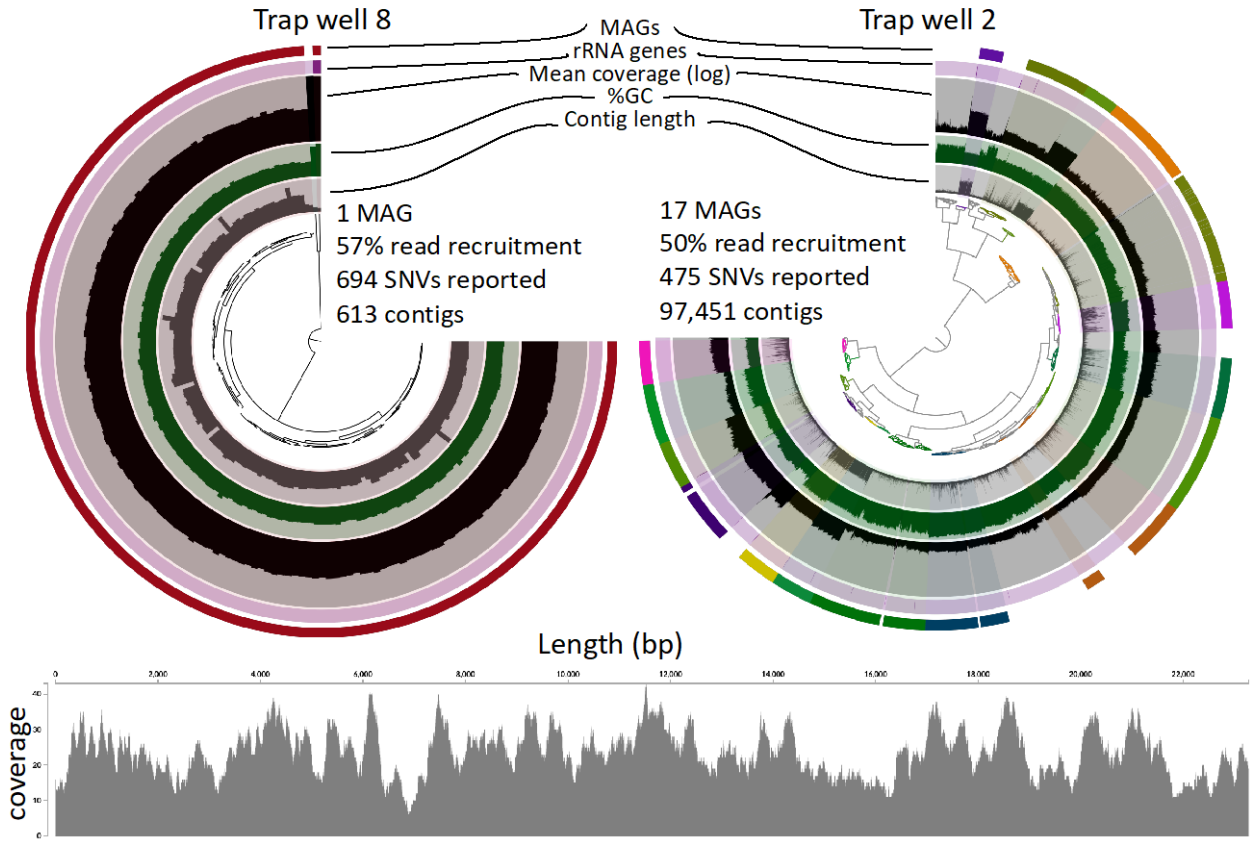

Figure 6. Comparison of MAGs from two traps. Each circular display contains a tree at the center representing the similarity of tetranucleotide frequency and coverage of each contig in the two independent assemblies. Subsequent layers demonstrate 1) contig length, 2) % GC content, 3) log mean coverage of the contig within the sample, 4) an indicator of whether a 16s rRNA gene was detected in the sample and 5) the bin location of the MAG collection. The coverage profile (bottom) shows an example of one 22 kbp contig derived from one of the MAGs. Any variation in the consensus of short reads mapping back to this contig would be highlighted and absence of any variation indicates that the short reads completely agree with the consensus.

The number of MAGs identified within the traps was highly correlated with the number of ASVs detected, and the relationship between the number of ASVs and MAGs was linear, with nearly three times the number of ASVs observed for every MAG (Figure 7).

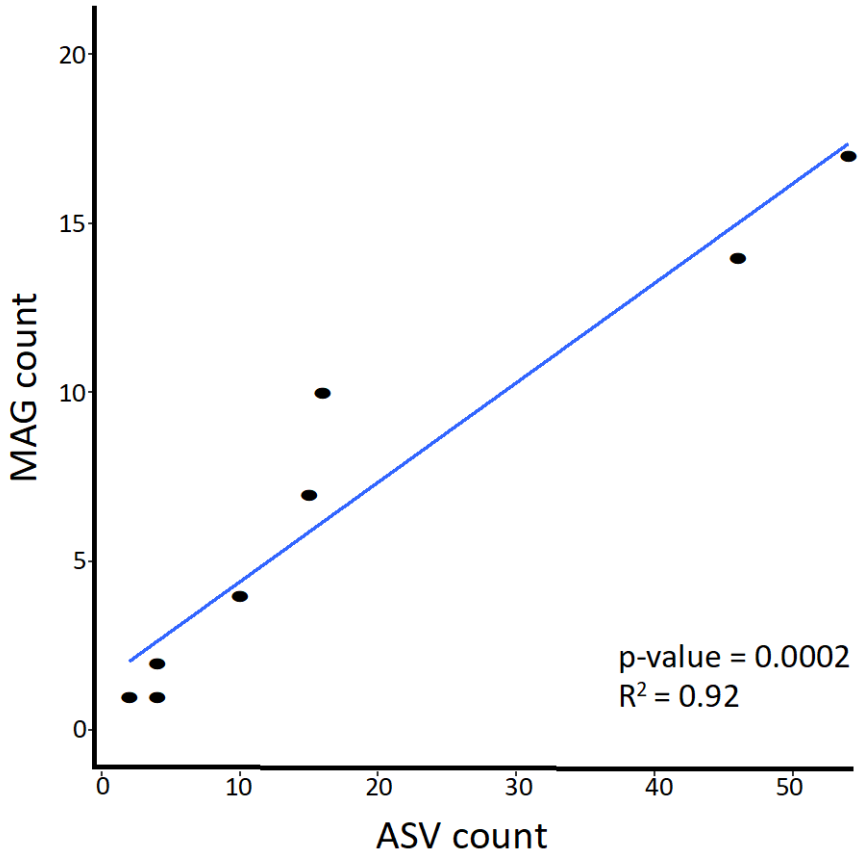

Figure 7. Linear model describing the relationship between the number of ASVs and MAGs recovered from each trap well.

This could result from the presence of multiple operons of the 16S rRNA gene within several of the genomes. This result indicates that 16S rRNA amplicon sequencing may overestimate the number of organisms isolated in each well, and estimates can be improved by metagenomic sequencing and genome reconstruction. We recovered ASVs and MAGs that could not be assigned taxonomy to the family level, indicating that they represent novel organisms. Obtaining genomic information for these organisms is a significant step toward understanding their functional capacity and provides us with the culture collections to validate their physiological potential. This system

271 offers a considerable improvement to classical approaches of dilution to extinction and streaking
272 plates because it allows for the capture of communities and strains in-situ with the potential to use
273 multiple media types in the same trap.

Acknowledgment

This material is based upon work supported by the National Science Foundation under grant no. IDBR 1353853. Support for the amplicon and metagenomic sequencing was provided by NSF grant no. DEB 1350491 to JLB. PIE LTER, where these samples were collected, is supported by NSF Grant no. OCE 1637630. EDG has a financial interest in the trap technology. Traps can be obtained by researchers through Microbial Devices, LLC.

References

[1] "Microbiology by numbers," *Nature Reviews Microbiology*, vol. 9, p. 628, 2011.

[2] J. T. Staley and A. Konopka, "Measurement of in situ activities of nonphotosynthetic microorganisms in aquatic and terrestrial habitats," *Annual Review of Microbiology*, vol. 39, no. 1, pp. 321–346, 1985.

[3] G. Yim, H. M. H. Wang, and J. Davies, "Antibiotics as signalling molecules," *Philosophical Transactions of the Royal Society B-Biological Sciences*, vol. 362, no. 1483, pp. 1195–1200, 2007.

[4] W. J. Watterson *et al.*, "Droplet-based high-throughput cultivation for accurate screening of antibiotic resistant gut microbes," *eLife*, vol. 9, pp. 1–22, Jun. 2020, doi: 10.7554/eLife.56998.

[5] Y. J. Eun, A. S. Utada, M. F. Copeland, S. Takeuchi, and D. B. Weibel, "Encapsulating bacteria in agarose microparticles using microfluidics for high-throughput cell analysis and isolation," *ACS Chemical Biology*, vol. 6, no. 3, pp. 260–266, Mar. 2011, doi: 10.1021/cb100336p.

[6] M. M. Villa *et al.*, "High-throughput isolation and culture of human gut bacteria with droplet microfluidics," *bioRxiv*, 2019, doi: 10.1101/630822.

[7] K. Leung *et al.*, "A programmable droplet-based microfluidic device applied to multiparameter analysis of single microbes and microbial communities," 2012, doi: 10.1073/pnas.1106752109/-/DCSupplemental.

[8] R. A. Bamford, A. Smith, J. Metz, G. Glover, R. W. Titball, and S. Pagliara, "Investigating the physiology of viable but non-culturable bacteria by microfluidics and time-lapse microscopy," *BMC Biology*, vol. 15, no. 1, Dec. 2017, doi: 10.1186/s12915-017-0465-4.

[9] Y. Lu, J. Gao, D. D. Zhang, V. Gau, J. C. Liao, and P. K. Wong, "Single cell antimicrobial susceptibility testing by confined microchannels and electrokinetic loading," *Analytical Chemistry*, vol. 85, no. 8, pp. 3971–3976, Apr. 2013, doi: 10.1021/ac4004248.

[10] A. Y. L. Jiang *et al.*, "High-throughput continuous dielectrophoretic separation of neural stem cells," *Biomicrofluidics*, vol. 13, no. 6, Nov. 2019, doi: 10.1063/1.5128797.

[11] L. D'Amico, N. J. Ajami, J. A. Adachi, P. R. C. Gascoyne, and J. F. Petrosino, "Isolation and concentration of bacteria from blood using microfluidic membraneless dialysis and dielectrophoresis," *Lab on a Chip*, vol. 17, no. 7, pp. 1340–1348, 2017.

[12] W. A. Braff, D. Willner, P. Hugenholtz, K. Rabaey, and C. R. Buie, "Dielectrophoresis-Based Discrimination of Bacteria at the Strain Level Based on Their Surface Properties," *PLOS ONE*, vol. 8, no. 10, pp. e76751–, Aug. 2013.

[13] P. Dow, K. Kotz, S. Gruszka, J. Holder, and J. Fiering, "Acoustic separation in plastic microfluidics for rapid detection of bacteria in blood using engineered bacteriophage," *Lab on a Chip*, vol. 18, no. 6, pp. 923–932, Mar. 2018, doi: 10.1039/c7lc01180f.

[14] W.-H. Chang *et al.*, "Rapid isolation and diagnosis of live bacteria from human joint fluids by using an integrated microfluidic system," *Lab on a Chip*, vol. 14, no. 17, pp. 3376–3384, 2014.

[15] S. Miller, A. A. Weiss, W. R. Heineman, and R. K. Banerjee, "Electroosmotic flow driven microfluidic device for bacteria isolation using magnetic microbeads," *Scientific Reports*, vol. 9, no. 1, Dec. 2019, doi: 10.1038/s41598-019-50713-z.

[16] D. Nichols *et al.*, "Use of ichip for high-throughput in situ cultivation of 'uncultivable microbial species,'" *Applied and Environmental Microbiology*, vol. 76, no. 8, pp. 2445–2450, Apr. 2010, doi: 10.1128/AEM.01754-09.

[17] A. Yoshiteru, K. Tomoyuki, H. Toru, O. Hiroaki, O. Haruko, and T. Satoshi, "Hollow-Fiber Membrane Chamber as a Device for In Situ Environmental Cultivation," *Applied and Environmental Microbiology*, vol. 75, no. 11, pp. 3826–3833, Jun. 2009, doi: 10.1128/AEM.02542-08.

[18] B. Berdy, A. L. Spoering, L. L. Ling, and S. S. Epstein, "In situ cultivation of previously uncultivable microorganisms using the ichip," *Nature Protocols*, vol. 12, no. 10, pp. 2232–2242, Oct. 2017, doi: 10.1038/nprot.2017.074.

[19] C. B. Raub, C. Lee, and E. Kartalov, "Sequestration of bacteria from whole blood by optimized microfluidic cross-flow filtration for Rapid Antimicrobial Susceptibility Testing," *Sensors and Actuators, B: Chemical*, vol. 210, pp. 120–123, 2015, doi: 10.1016/j.snb.2014.10.061.

[20] X. Fan *et al.*, "A microfluidic chip integrated with a high-density PDMS-based microfiltration membrane for rapid isolation and detection of circulating tumor cells," *Biosensors and Bioelectronics*, vol. 71, pp. 380–386, Sep. 2015, doi: 10.1016/j.bios.2015.04.080.

[21] S. Zelenin, J. Hansson, S. Ardabili, H. Ramachandraiah, H. Brismar, and A. Russom, "Microfluidic-based isolation of bacteria from whole blood for sepsis diagnostics," *Biotechnology Letters*, vol. 37, no. 4, pp. 825–830, Apr. 2015, doi: 10.1007/s10529-014-1734-8.

[22] Z. Wu, B. Willing, J. Bjerketorp, J. K. Jansson, and K. Hjort, "Soft inertial microfluidics for high throughput separation of bacteria from human blood cells," *Lab on a Chip*, vol. 9, no. 9, pp. 1193–1199, 2009, doi: 10.1039/b817611f.

[23] J. Männik, R. Driessen, P. Galajda, J. E. Keymer, and C. Dekker, "Bacterial growth and motility in sub-micron constrictions," *Proceedings of the National Academy of Sciences*, vol. 106, no. 35, p. 14861, Aug. 2009.

[24] N. Tandogan, P. N. Abadian, S. Epstein, Y. Aoi, and E. D. Goluch, "Isolation of microorganisms using sub-micrometer constrictions," *PLoS ONE*, vol. 9, no. 6, Jun. 2014, doi: 10.1371/journal.pone.0101429.

[25] H. Rezaei Nejad *et al.*, "Ingestible Osmotic Pill for In Vivo Sampling of Gut Microbiomes," *Advanced Intelligent Systems*, vol. 1, no. 5, p. 1900053, Sep. 2019, doi: 10.1002/aisy.201900053.

[26] M. L. Sogin *et al.*, "Microbial diversity in the deep sea and the underexplored "rare biosphere"," *Proceedings of the National Academy of Sciences*, vol. 103, no. 32, p. 12115, Aug. 2006.

[27] D.-L. Sun, X. Jiang, Q. L. Wu, and N.-Y. Zhou, "Intragenomic Heterogeneity of 16S rRNA Genes Causes Overestimation of Prokaryotic Diversity," *Applied and Environmental Microbiology*, vol. 79, no. 19, p. 5962, Aug. 2013.

[28] S. M. Huse, L. Dethlefsen, J. A. Huber, D. M. Welch, D. A. Relman, and M. L. Sogin, "Exploring Microbial Diversity and Taxonomy Using SSU rRNA Hypervariable Tag Sequencing," *PLOS Genetics*, vol. 4, no. 11, pp. e1000255–, Aug. 2008.

[29] H. Krehenwinkel, M. Wolf, J. Y. Lim, A. J. Rominger, W. B. Simison, and R. G. Gillespie, "Estimating and mitigating amplification bias in qualitative and quantitative arthropod metabarcoding," *Scientific Reports*, vol. 7, no. 1, p. 17668, 2017.

[30] N. R. Pace, "Mapping the tree of life: progress and prospects," *Microbiology and molecular biology reviews : MMBR*, vol. 73, no. 4, pp. 565–576, 2009.

[31] L. A. Hug *et al.*, "A new view of the tree of life," *Nature Microbiology*, vol. 1, p. 16048, 2016.

[32] T. B. Britschgi and R. D. Fallon, "PCR-amplification of mixed 16S rRNA genes from an anaerobic, cyanide-degrading consortium," *FEMS Microbiology Ecology*, vol. 13, no. 3, pp. 225–231, Aug. 1994.

[33] J. G. Caporaso *et al.*, "Global patterns of 16S rRNA diversity at a depth of millions of sequences per sample," *Proceedings of the National Academy of Sciences*, vol. 108, no. Supplement 1, p. 4516, 2011.

[34] B. J. Callahan, P. J. McMurdie, M. J. Rosen, A. W. Han, A. J. A. Johnson, and S. P. Holmes, "DADA2: High-resolution sample inference from Illumina amplicon data," *Nature Methods*, vol. 13, no. 7, pp. 581–583, 2016.

[35] A. M. Eren, J. H. Vineis, H. G. Morrison, and M. L. Sogin, "A Filtering Method to Generate High Quality Short Reads Using Illumina Paired-End Technology," *PLOS ONE*, vol. 8, no. 6, p. e66643, 2013.

[36] A. Bankevich *et al.*, "SPAdes: a new genome assembly algorithm and its applications to single-cell sequencing," *Journal of computational biology : a journal of computational molecular cell biology*, vol. 19, no. 5, pp. 455–477, 2012.

[37] B. Langmead and S. L. Salzberg, "Fast gapped-read alignment with Bowtie 2," *Nature Methods*, vol. 9, no. 4, pp. 357–359, 2012.

[38] A. M. Eren *et al.*, "Anvi'o: an advanced analysis and visualization platform for `omics data," *PeerJ*, vol. 3, p. e1319, 2015.

[39] D. Hyatt, G.-L. Chen, P. F. LoCascio, M. L. Land, F. W. Larimer, and L. J. Hauser, "Prodigal: prokaryotic gene recognition and translation initiation site identification," *BMC Bioinformatics*, vol. 11, no. 1, p. 119, 2010.

[40] B.-J. Yoon, "Hidden Markov Models and their Applications in Biological Sequence Analysis," *Current genomics*, vol. 10, no. 6, pp. 402–415, 2009.

[41] L. Pritchard, R. H. Glover, S. Humphris, J. G. Elphinstone, and I. K. Toth, "Genomics and taxonomy in diagnostics for food security: soft-rotting enterobacterial plant pathogens," *Analytical Methods*, vol. 8, no. 1, pp. 12–24, 2016.

[42] B. Buchfink, C. Xie, and D. H. Huson, "Fast and sensitive protein alignment using DIAMOND," *Nature Methods*, vol. 12, no. 1, pp. 59–60, 2015.

[43] D. H. Parks *et al.*, "A standardized bacterial taxonomy based on genome phylogeny substantially revises the tree of life," *Nature Biotechnology*, vol. 36, no. 10, pp. 996–1004, 2018.

[44] J. L. Bowen, H. G. Morrison, J. E. Hobbie, and M. L. Sogin, "Salt marsh sediment diversity: a test of the variability of the rare biosphere among environmental replicates," *The ISME Journal*, vol. 6, no. 11, pp. 2014–2023, 2012.

[45] P. J. Kearns, J. H. Angell, E. M. Howard, L. A. Deegan, R. H. R. Stanley, and J. L. Bowen, "Nutrient enrichment induces dormancy and decreases diversity of active bacteria in salt marsh sediments," *Nature Communications*, vol. 7, no. 1, p. 12881, 2016.

[46] R. M. Bowers *et al.*, "Minimum information about a single amplified genome (MISAG) and a metagenome-assembled genome (MIMAG) of bacteria and archaea," *Nature Biotechnology*, vol. 35, no. 8, pp. 725–731, 2017.